

Online Supplement

RNA is Favorable for Analyzing *EGFR* Mutations in Malignant Pleural Effusion of Lung Cancer

Tzu-Hsiu Tsai, Kang-Yi Su, Shang-Gin Wu, Yih-Leong Chang, Sheng-Ching Luo,
I-Shiow Jan, Chong-Jen Yu, Sung-Liang Yu, Jin-Yuan Shih, and Pan-Chyr Yang

METHODS

Cell lines

A NSCLC cell line with in-frame deletion in exon 19, H1650 (ATCC number: CRL-5883), and a transformed mesothelial cell line, Met-5A (ATCC number: CRL-9444), were used to illustrate the relative expression of *EGFR* between tumor and reactive mesothelial cells. These two cells were also used for cell-line mixing study (see below).

Immunocytochemical analysis of effusion cell blocks

To provide an estimate of tumor cellular percentages within samples of MPE, as well as their relationship with the yields of *EGFR*-mutation detection by different assay modalities, we performed immunocytochemical analysis for cell-block preparations of 29 MPE samples. The sections of cell blocks were immunostained with a monoclonal antibody to 8G7G3/1 TTF-1 (1:200; Dako Corporation, Carpinteria, CA, USA) and counterstained with hematoxylin. The positively-stained tumor cells were estimated to account for <5% to 70% of total nucleated cells within these MPEs. The sections were also immunostained with a monoclonal antibody to calretinin (1:100; Leica Biosystems, Newcastle, Newcastle-upon-tyne, UK), a marker of mesothelial cells, to evaluate the relative contamination by reactive mesothelial cells in these fluid samples. Mesothelial cells were estimated to constitute 0-25% of total nucleated cells within MPEs.

Real-time quantitative RT-PCR

The expressions of *EGFR* of two cell lines, H1650 and Met-5A, and cells from 29 MPEs of lung adenocarcinoma and from 20 benign pleural effusions were determined with real-time RT-PCR using the TaqMan EZ RT-PCR Core Reagents and the Applied Biosystems 7500 Real-time PCR System (Applied Biosystems, Foster City, CA, USA). Thermal cycling conditions were 2 minutes at 50°C, 30 minutes at 60°C and 5 minutes at

95°C, followed by 40 cycles of 15 seconds at 95°C and 1 minute at 60°C. The sequences of primers and detection probes for real-time quantitative RT-PCR were 5'-CGCAAAGGGCATGAACTACTT-3' (forward), 5'-CTTGACATGCTGCGGTGTTT-3' (reverse), and (FAM)TGCACCGCGACCTGGCAGC(TAMRA) (detection probe).

Cell-line mixing study

We performed a cell-line mixing study to demonstrate the effect of using RNA as template to enrich mutant *EGFR* from tumor cells for sensitive mutation detection. H1650 cells (with deletion 2235-2249 in exon 19) were mixed with Met-5A mesothelial cells in different extent, followed by sequencing analysis using isolated RNA as the template. The limit of mutation detection was defined as the lowest dilution fold while the signal of mutant allele could be recognized on the sequencing chromatogram. The isolation of RNA, RT-PCR, and direct sequencing were as described previously in the METHODS of this article.

Analysis of *EGFR* mutations with the Scorpion Amplified Refractory Mutation System (SARMS) method

Analysis of *EGFR* mutations with the Scorpion Amplified Refractory Mutation System (SARMS) method was conducted using the EGFR RGQ PCR Kit (Qiagen, Valencia, CA, USA). This kit combines two technical methods, Scorpion and ARMS, to detect 29 *EGFR* mutations in real-time PCRs with the detection limit of 1%. Assays were carried out according to the manufacturer's protocol and using the Rotor-Gene Q real-time PCR system (Qiagen), with data analysis using the Rotor-Gene Q software (version 2.0.2). These PCRs were performed in duplicate for each sample.

Table S1. Primers for amplification of exon 18, 19, 20 and 21 of *EGFR* from genomic DNA

Exon	External (5'-3')	Nested (5'-3')
18	F: CAAATGAGCTGGCAAGTGCCGTGTC R: GAGTTTCCCAAACACTCAGTGAAAC	F: CAAGTGCCGTGTCCTGGCACCCAAGC R: CCAAACACTCAGTGAAACAAAGAG
19	F: AAATAATCAGTGTGATTCGTGGAG R: GAGGCCAGTGCTGTCTCTAAGG	F: GTGCATCGCTGGTAACATCC R: TGTGGAGATGAGCAGGGTCT
20	F: CCATGAGTACGTATTTTGAAACTC R: CATATCCCATGGCAAACCTTTGC	F: GAAACTCAAGATCGCATTTCATGC R: GCAAACCTTTGCTATCCCAGGAG
21	F: GCAGCGGGTTACATCTTCTTTC R: CAGCTCTGGCTCACACTACCAG	F: GCTCAGAGCCTGGCATGAA R: CATCCTCCCCTGCATGTGT

Table S2. PCR primers and detection probes used for the identification of T790M, L858R and exon 19 deletions by MALDI-TOF MS analysis

	Targeted mutation	Sequence (5'-3')	Mass (Da)
T790M			
PCR primer		F: ACGTTGGATGATCTGCCTCACCTCCACCGT R: ACGTTGGATGGCCGAAGGGCATGAGCTGC	--
Detection probe	2369 C>T	TGCCTCACCTCCACCGTGCAGCTCATCA	8405.5
L858R			
PCR primer		F: ACGTTGGATGACGTACTGGTGAAAACACCG R: ACGTTGGATGCGCACCCAGCAGTTTGGCC	--
Detection probe	2573 T>G	AAGATCACAGATTTTGGGC	5851.8
Exon 19 deletions			
PCR primer		F: ACGTTGGATGGAAAGTTAAAATTCCCGTCGC R: ACGTTGGATGTCACATCGAGGATTCCTTG	--
Detection probe			
PW	Wild-type	TCGCTATCAAGGAAT	4576.0
P1	Del2235-2249	ATCCCGTCGCTATCAA	5105.3
P2	Del2236-2250	CATTCCCGTCGCTATCAAG	5723.7
P3/4	Del2237-2251	AAAATTCCCGTCGCTATCAAGG	6703.4
	Del2237-2255		
P5/6	Del2239-2248	ATCCCGTCGCTATCAAGGAACCA	7281.8
	Del2239-2251		
P7	Del2239-2256	AAAATTCCCGTCGCTATCAAGGAACC	7908.2
P8/9	Del2240-2254	CGTCGCTATCAAGGAATC	5483.6
	Del2240-2257		

PCR, polymerase chain reaction; MALDI-TOF MS,

matrix-assisted-laser-desorption-ionization time-of-flight mass spectrometry.

Table S3. Basic data and response to first-line EGFR TKIs in patients with mutations other than L858R and exon 19 deletions

Gender	Smoking	<i>EGFR</i> mutations		Clinical response
		gDNA/sequencing	RNA/sequencing	
M	Non-smoker	L747P	L747P	PD
F	Non-smoker	S768I	G719A + S768I	PD
F	Non-smoker	--	R776H + L861Q	PD
M	Non-smoker	--	K806E	PR
F	Non-smoker	767-769 dup ASV	767-769 dup ASV	PD
F	Non-smoker	L861Q	G719S + L861Q	PR
F	Smoker	--	D770_N771 insG	PD
F	Non-smoker	--	E746G + L861Q	PR
M	Smoker	L861Q	L861Q	SD

gDNA, genomic DNA; M, male; F, female; PR, partial response; SD, stable disease; PD, progressive disease.

Table S4. The estimated tumor cellular percentages and yields of *EGFR*-mutation detection by different assay modalities

Sample no.	Tumor cell %	DNA/sequencing	DNA/MALDI-TOF MS	RNA/sequencing
Tumor cell percentage >50%				
1	70%	L858R	L858R	L858R
2	60%	L858R	L858R	L858R
3	60%	Del 19	Del 19	Del 19
4	60%	L858R	L858R	L858R
5 ^{*#}	60%	L861Q	Wild	L861Q
6	55%	L858R	L858R	L858R
7	55%	L858R	L858R	L858R
Tumor cell percentage 25~50%				
8	50%	Wild	Wild	Wild
9	40%	Del 19	Del 19	Del 19
10	40%	L858R	L858R	L858R
11	40%	Del 19	Del 19	Del 19
12	40%	Del 19	Del 19	Del 19
13 ^{*#}	30%	Del 19	Wild	Del 19
14	30%	Wild	Wild	Wild
15	30%	Del 19	Del 19	Del 19
16	30%	L858R	L858R	L858R
Tumor cell percentage 15~25%				
17 ^{*#}	25%	Wild	Wild	L858R
18	20%	Del 19	Del 19	Del 19
19	20%	Wild	Wild	Wild
Tumor cell percentage 5~15%				
20 [*]	15%	Wild	Wild	L858R
21 [*]	10%	Wild	L858R	L858R
22	10%	L858R	L858R	L858R
23	6%	L858R	L858R	L858R
24	5%	Del 19	Del 19	Del 19
25	5%	Wild	Wild	Wild
26	5%	Wild	Wild	Wild

Continued

Tumor cell percentage <5%				
27	<5%	Wild	Wild	Wild
28	<5%	Del 19	Del 19	Del 19
29*	<5%	Wild	Wild	L858R

* Samples with discordant results of *EGFR* status assessed by different analytical methods.

Cases with *EGFR* mutations beyond the scope of detection by probes designed for MALDI-TOF MS analysis. The L858R mutation in sample no. 17 was 2572-2573 CT>AG. MALDI-TOF MS, matrix-assisted-laser-desorption-ionization time-of-flight mass spectrometry; Del 19, deletions in exon 19.

FIGURE LEGENDS

Figure S1. Illustration of probes for the detection of T790M (2369 C>T), L858R (2573 T>G) and the nine variants of deletions in exon 19 by MALDI-TOF MS analysis.

Red line indicates the probe sequences homologous to the *EGFR* endogeneous nucleotides. In panel A and B, the red letter indicates the 2369 nucleotide substitution from C to T of T790M in exon 20 (panel A) and the 2573 nucleotide substitution from T to G of L858R in exon 21 (panel B). In panel C, the sequences indicate different in-frame deletions in exon 19. Note that for assembling each detection probes equally distributed on the mass spectrum, additional mismatched nucleotides are extended for some probes (shown as red letters).

Figure S2. Expressions of *EGFR* mRNA between NSCLC (H1650) and mesothelial (Met-5A) cells, as well as between malignant and benign pleural effusions.

To demonstrate that NSCLC cells have higher *EGFR* expression than reactive mesothelial cells, we compared the levels of *EGFR* mRNA between a NSCLC cell line (H1650) and a transformed mesothelial cell line (Met-5A). The expression of *EGFR* in H1650 cells is approximately four times higher than that in Met-5A cells (panel A). Moreover, *EGFR* expression of cells from 29 MPEs of lung adenocarcinoma is significantly higher than that from 20 benign pleural effusions ($P=0.02$) (panel B). These results support that the expression of *EGFR* is remarkably different between tumor and nontumor cells within samples of MPE. TBP, TATA-binding protein; BPE, benign pleural effusion; MPE, malignant pleural effusion.

Figure S3. Sequencing chromatograms of the cell-line mixing study.

H1650 cells (with deletion 2235-2249 in exon 19) were mixed in different extent with Met-5A mesothelial cells, followed by *EGFR* sequencing analysis using isolated RNA as the template. Tracings are in the forward direction. Horizontal arrows are shown to demonstrate the breakpoint of the deletions. The minimal proportion of H1650 among Met-5A cells for which the signal of mutant allele could be apparently recognized is 3% (i.e., Met-5A:H1650 = 1:0.03). Considering the detection limit of 15-25% by direct sequencing, this result illustrates the remarkable effect of using RNA as template to enrich mutant *EGFR* from tumor cells for sensitive mutation analysis.

Figure S1.

A

2340 2350 2360 2370 2380
 ATCTGCCTCACCTCCACCGTGCAGCTCATCACGCAGCTCATGCCCTTCG wild-type
 ATCTGCCTCACCTCCACCGTGCAGCTCATCATGCAGCTCATGCCCTTCG T790M
T790M Detection probe

B

2540 2550 2560 2570 2580
 CACCGCAGCATGTCAAGATCACAGATTTTGGGCTGGCCAAACTGCTGGG wild-type
 CACCGCAGCATGTCAAGATCACAGATTTTGGGC GGCCAAACTGCTGGG L858R
L858R Detection probe

C

2220 2230 2240 2250 2260
 AATCCCGTCGCTATCAAGGAATTAAGAGAAGCAACATCTCCGAAAGCCA wild-type
PW
P1 AATCCCGTCGCTATCAA AACATCTCCGAAAGCCA del 2235-2249
P2 C AATCCCGTCGCTATCAAG ACATCTCCGAAAGCCA del 2236-2250
P3/4 AA AATCCCGTCGCTATCAAGG CATCTCCGAAAGCCA del 2237-2251
 AATCCCGTCGCTATCAAGG TTCCGAAAGCCA del 2237-2255
P5/6 AATCCCGTCGCTATCAAGGAA CCAACATCTCCGAAAGCCA del 2239-2248
 AATCCCGTCGCTATCAAGGAA CCATCTCCGAAAGCCA del 2239-2251
P7 AA AATCCCGTCGCTATCAAGGAA CCGAAAGCCA del 2239-2256
P8/9 AATCCCGTCGCTATCAAGGAAT CTCCGAAAGCCA del 2240-2254
 AATCCCGTCGCTATCAAGGAAT CGAAAGCCA del 2240-2257

Figure S2.

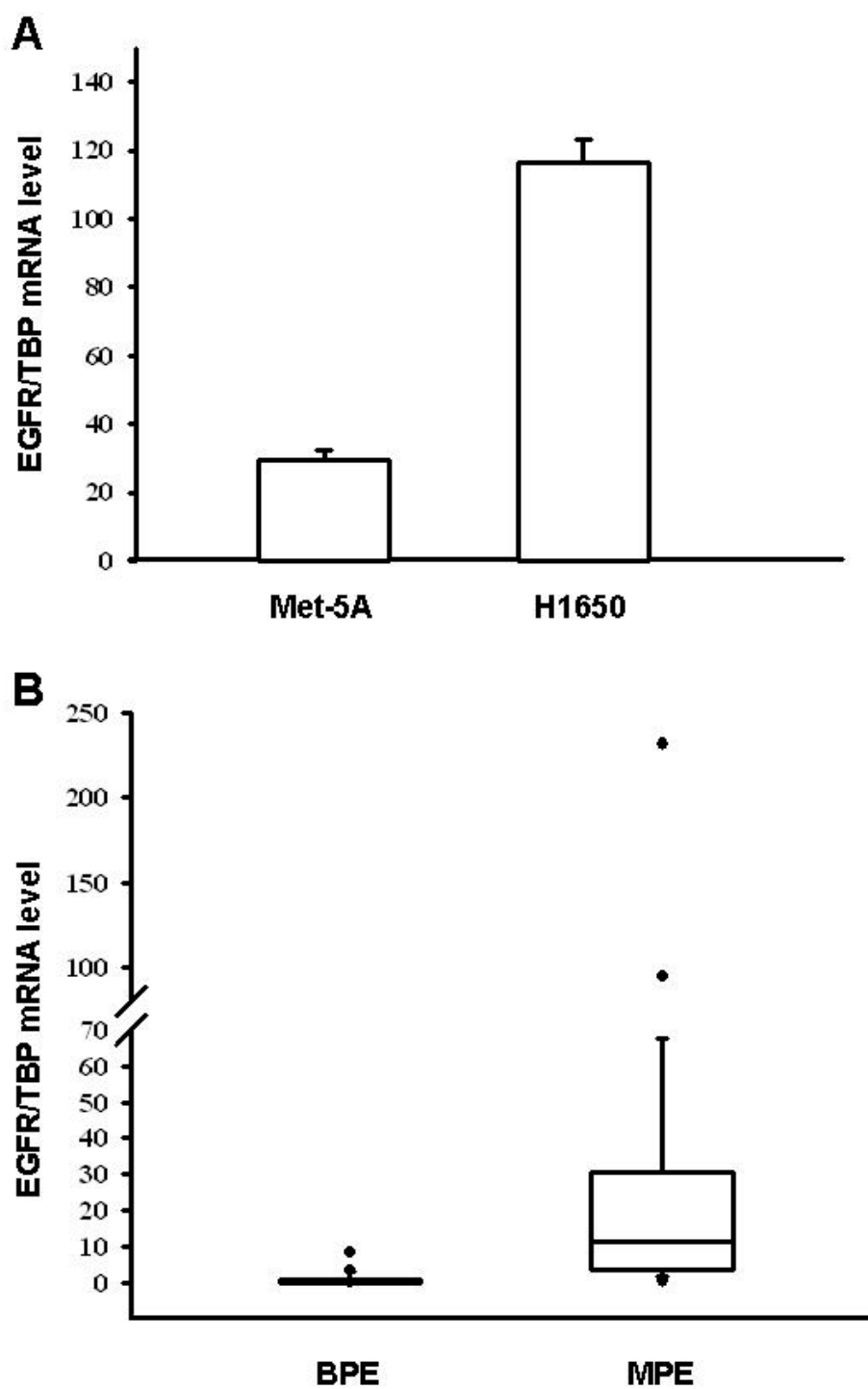


Figure S3.

